Journal of the Mechanical Behavior of Biomedical Materials 100 (2019) 103366

Contents lists available at ScienceDirect

Journal of the Mechanical Behavior of Biomedical Materials

journal homepage: www.elsevier.com/locate/jmbbm

Zinc oxide and copper nanoparticles addition in universal adhesive systems improve interface stability on caries-affected dentin

Mario Felipe Gutiérrez[a,b,c], Jorge Bermudez[a], Andrés Dávila-Sánchez[a,d], Luisa F. Alegría-Acevedo[a,e], Luján Méndez-Bauer[a], Marcela Hernández[f], Jessica Astorga[f], Alessandra Reis[a], Alessandro D. Loguercio[a,*], Paulo V. Farago[g], Eduardo Fernández[h,i]

[a] Department of Restorative Dentistry, School of Dentistry, State University of Ponta Grossa, Ponta Grossa, Brazil
[b] Institute for Research in Dental Sciences, Faculty of Dentistry, University of Chile, Santiago, Chile
[c] Facultad de Odontología, Universidad Finis Terrae, Chile
[d] Department of Restorative Dentistry and Biomaterials, San Francisco de Quito University, Quito, Ecuador
[e] Universidad Politécnica y Artística del Paraguay, Paraguay
[f] Department of Oral Pathology and Medicine and Laboratory of Periodontal Biology, Faculty of Dentistry, University of Chile, Santiago, Chile
[g] Department of Pharmaceutical Sciences, State University of Ponta Grossa, Ponta Grossa, Brazil
[h] Department of Restorative Dentistry, Faculty of Dentistry, University of Chile, Chile
[i] Instituto de Ciencias Biomédicas, Universidad Autónoma de Chile, Santiago, Chile

ARTICLE INFO

Keywords:
Universal adhesive system
Zinc oxide
Copper
Nanoparticles
Microtensile bond strength
Nanoleakage

ABSTRACT

This study evaluated the MMP inhibition of the zinc oxide and copper nanoparticles (ZnO/CuNp), and the effects of their addition into adhesives on antimicrobial activity (AMA), ultimate tensile strength (UTS), *in vitro* degree of conversion (*in vitro*-DC), as well as, resin–dentin bond strength (μTBS), nanoleakage (NL) and *in situ*-DC on caries-affected dentin. Anti-MMP activity was evaluated for several MMPs. ZnO/CuNp (0% [control]; 5/0.1 and 5/0.2 wt%) were added into Prime&Bond Active (PBA) and Ambar Universal (AMB). The AMA was evaluated against *Streptococcus mutans*. UTS were tested after 24 h and 28d. After induced caries, adhesives and composite were applied to flat dentin surfaces, and specimens were sectioned to obtain resin–dentin sticks. μTBS, NL, *in vitro*-DC and *in situ*-DC were evaluated after 24 h. ANOVA and Tukey's test were applied ($\alpha = 0.05$). ZnO/CuNp demonstrated anti-MMP activity ($p < 0.05$). The addition of ZnO/CuNp increased AMA and UTS (AMB; $p < 0.05$). UTS for PBA, *in vitro*-DC, *in situ*-DC and μTBS for both adhesives were maintained with ZnO/CuNp ($p > 0.05$). However, lower NL was observed for ZnO/CuNp groups ($p < 0.05$). The addition of ZnO/CuNp in adhesives may be an alternative to provide antimicrobial, anti-MMP activities and improves the integrity of the hybrid layer on caries-affected dentin.

1. Introduction

Dental caries is one of the most common chronic oral diseases throughout the world with immense social-economic impact. It is characterized by acid demineralization and degeneration of organic matrix on the tooth surface that can result in the cavities formation (Selwitz et al., 2007). Currently, partial caries removal appears as the best minimally invasive strategy for cavitated carious lesions, in order to conserve tooth structure and avoid the risk of injury to the pulp (FDI, 2017). For that, only the superficial opaque zone of caries-infected dentin is removed, and a deeper and partially demineralized zone of caries-affected dentin, that is remineralizable and not yet colonized by bacteria, is preserved (de Almeida Neves et al., 2011; Wambier et al., 2007).

Caries-affected dentin has a low mineral content, an altered cross-striated pattern of organic matrix of the collagen fibrils and non-collagenous proteins, and an increased porosity (Tjäderhane et al., 2015), resulting in increased dentin humidity and significantly reduced dentin mechanical properties (Tjäderhane, 2019). Thus, hybrid layers created in caries-affected dentin exhibit lower bond strength and durability than sound dentin regardless of the adhesive system used (Isolan et al., 2018). Besides this, bonding to caries-affected dentin degraded much faster than those created in sound dentin (Hebling et al., 2005). This occur because higher rate of different enzymes expression and/or

* Corresponding author. Universidade Estadual de Ponta Grossa, Departamento de Odontologia, Avenida Carlos Cavalcanti, 4748 – Uvaranas, Ponta Grossa, Paraná, CEP: 84030-900, Brazil.
E-mail address: aloguercio@hotmail.com (A.D. Loguercio).

https://doi.org/10.1016/j.jmbbm.2019.07.024
Received 25 March 2019; Received in revised form 10 June 2019; Accepted 20 July 2019
Available online 04 August 2019
1751-6161/

activation in this caries-affected dentin when compared with sound dentin (Toledano et al., 2010), in response to the intermittent pH fluctuations produced during caries progression, that permit enzymatic activation and promoting collagen degradation (Chaussain-Miller et al., 2006). Thus, adhesive restorations on caries-affected dentin is challenging for clinicians, and what is worse, to date relatively limited information exists about the bonding process to this clinically relevant substrate (Marangos et al., 2009).

On the other hand, the exposition of lactic acid produced by *S. mutans* during the occurrence of primary or secondary caries, reduces mechanical properties and fracture resistance of dentin at lower mastication forces (Orrego et al., 2017). This is why the development of materials with antibacterial and enzymatic inhibitors properties becomes so important, in order to increase the durability of the adhesive/dentin interface, without compromising the mechanical properties of the adhesive (Cocco et al., 2015).

In this sense, metallic nanoparticles have been highlighted among the most promising agents with antibacterial properties, exhibiting biocidal activities at low concentrations (Palza, 2015). Copper nanoparticles (CuNp) have been shown to be effective against gram-positive and gram-negative bacteria (Schrand et al., 2010). In addition to important antimicrobial activity, copper is cheap, so the synthesis of copper nanoparticles has a better cost-benefit ratio. Also, CuNp seems to be a potent inhibitor of dentin MMP-2 (metalloprotease-2), and to stimulate the secretion of tissue inhibitors of MMPs, causing a lower degradation pattern in the resin/dentin interface (de Souza et al., 2000). Otherwise, zinc oxide nanoparticles (ZnONp) can promote subtle conformational changes in collagenase cleavage sites of collagen molecules that protects collagen from MMPs' activity (Osorio et al., 2011).

Recent studies showed that the addition of CuNp in concentrations up to 0.1 wt% in an adhesive system provides antimicrobial properties and preserves the bonding to dentin after 1- and 2-year of water storage, without reducing the mechanical properties of the adhesive formulations (Gutierrez et al., 2017a, 2017b). On the other hand, a recent study showed that the addition of ZnONp in concentration of 5 wt% into a dental adhesive increases its antimicrobial properties without affecting their bond strength (Saffarpour et al., 2016). Likewise, the incorporation of ZnONp in concentration of 1 wt% in an adhesive system preserves the bonding to dentin after 6-months, without reducing the mechanical properties of the adhesive (Barcellos et al., 2016). Moreover, formulations also resulted in the formation of apatite crystallites on the collagen fibrils, favoring dentin mineralization, reducing MMP-mediated collagen degradation (Toledano et al., 2012), may inhibit dentin demineralization (Takatsuka et al., 2005), and may promote enamel remineralization (Lynch et al., 2011). However, to extent of our knowledge, the effect of combination of zinc oxide and copper nanoparticles (ZnO/CuNp) incorporated in the same dental adhesive has never been evaluated, as well as, the properly concentration of each one. This is important, because any change in the well-balanced chemical composition of the universal adhesive systems could imply possible mechanical and physico-chemical failures, as well as biological hazards.

Therefore, considering the importance of studying the bonding procedures to caries-affected dentin, in order to find alternative approaches in the context of decreasing/retarding hybrid layer degradation, this *in vitro* study was designed to investigate the MMP inhibition of the ZnO/CuNp, and the effects of their addition in different concentrations into two commercial universal adhesive systems on the antimicrobial activity, ultimate tensile strength, *in vitro* degree of conversion, as well as, microtensile bond strength, nanoleakage, microleakage evaluation by confocal laser scanning microscopy and *in situ* degree of conversion in the resin-caries-affected dentin interface.

Table 1
Zinc oxide and Copper Nanoparticles Specifications.

Type of particles/batch number/ manufacturer	Specifications
Zinc oxide nanoparticles (ZnO)8410DL Skyspring Nanomaterials, Inc[a]	Purity: 99.8% trace metals basis Appearance: White-yellow nanopowder Average Particle Size: 10–30 nm Specific Surface Area: 30–50 m^2/g
Copper nanoparticles (Cu) 0820XH Skyspring Nanomaterials, Inc[a]	Purity: 99.9% trace metals basis Appearance: Black nanopowder Average Particle Size: 40–60 nm Specific Surface Area: ~12 m^2/g Morphology: spherical Bulk density: 0.19 g/cm^3 True density: 8.9 g/cm^3

[a] www.ssnano.com.

2. Materials and methods

2.1. Anti-MMP activity

In this study were used ZnONp and CuNp (SkySpring Nanomaterials, Inc., Houston, TX, USA; www.ssnano.com). The properties of ZnONp and CuNp are shown in Table 1. MMP activity assays were conducted using recombinant MMP-2, MMP-8 and MMP-9 with MMP fluorometric assay kits (SensoLyte assay kits; AnaSpec, Fremont, CA, USA) following manufacturer's recommendations. The ZnO/CuNp at concentrations of 5% zinc and 0.1% copper (5/0.1) and 5% zinc and 0.2% copper (5/0.2), and active MMPs (pre-incubated with 10 mM of amino-phenyl mercuric acetate (APMA)) were mixed with 5-FAM/QXLTM 520 fluorescence resonance energy transfer (FRET) peptide substrate in assay buffer using 96 well plates. For the intact FRET peptide, the fluorescence of 5-FAM was quenched by QXL 520. Upon cleavage into 2 separate fragments by MMPs, the fluorescence of 5-FAM was recovered and monitored at excitation/emission wavelengths (490/520 nm, respectively). After 1 h of incubation, the fluorescence signal was read by a micro-plate reader (Synergy HT; Bio-Tek Instrument Inc., Winooski, VT, USA) (Hashimoto et al., 2015) an expressed as relative fluorescent units (RFU). Diluted active MMPs were used as positive controls; 25 μM Ilomastat was used as inhibitor control, and test compound controls with no MMP were added to assess their autoimmunofluorescence. Six samples of each group were conducted for each MMP assay.

2.2. Formulation of the experimental adhesives

It was formulated experimental adhesives using two universal adhesive systems: Prime&Bond Active (Dentsply-Sirona, Konstanz, Baden-Württemberg, Germany) and Ambar Universal (FGM Prod. Odont. Ltda, Joinville, SC, Brazil). Six experimental adhesives systems were formulated according to the addition of different concentrations of ZnO and CuNp for each commercial universal adhesive (wt%): 0% (control, commercial material); 5/0.1% and 5/0.2%. The incorporation to the adhesive solution was done in a dark room with a motorized stirrer (Gutierrez et al., 2017b).

2.3. In vitro antimicrobial activity

Pure culture was obtained by culturing *Streptococcus mutans* (*S. mutans)* ATCC 25175 in brain heart infusion broth (BHI, Difco Laboratories, Detroit, MI, USA) for 72 h at 37 °C (Gutierrez et al., 2017b). Then, 100 μL of the bacterial suspension was swabbed onto BHI to create the lawn (Gregson et al., 2012; Huang et al., 2012). Disk diffusion method was used to measure *S. mutans* sensitivity to the adhesive groups (described in the last paragraph). Filter paper discs of

6 mm diameter were prepared from Whatman filter paper No. 1 (Sigma–Aldrich, Munich, Germany), placed in a Petri dish and sterilized in a hot air oven at 160 °C for 2 h. Thereafter, discs were impregnated according to the following: 1) with 20 μL of each of the experimental adhesive, evaporating the solvent and placed immediately over the plates, without polymerization; and 2) with 20 μL of each of the experimental adhesive, evaporating the solvent and light-cured for 20 s with a LED light source at 1000 mW/cm^2 (VALO, Ultradent Products, South Jordan, UT, USA), and placed immediately over the plates. The plates were incubated in an anaerobic jar (5% CO_2) for 48 h at 37 °C. The inhibition zones (mm) were measured with a digital caliper to the nearest 0.1 mm (Absolute Digimatic, Mitutoyo, Tokyo, Japan). Three samples of each adhesive groups were tested.

2.4. Ultimate tensile strength

A metallic matrix with an hourglass shape (10 mm long, 2 mm wide, 1 mm deep and a cross-sectional middle area of approximately 1.5 mm^2) was employed for the construction of the specimens. After isolating the metallic matrix with a very thin layer of petroleum jelly, we dispensed the adhesive until completely fill the mold. All visible air bubbles trapped in the adhesive specimens were carefully removed with a brush (Cavibrush, FGM Prod. Odont. Ltda, Joinville, SC, Brazil). An air stream was applied for solvent evaporation for 40 s at a distance of 10 cm.

Under a plastic matrix strip, the adhesive specimens were light-cured for 40 s with a LED light source at 1000 mW/cm^2 (VALO, Ultradent Products, South Jordan, UT, USA), in close contact with each hourglass-like specimen. After polymerization, the specimens were removed from the mold, and polished with 600-grit SiC paper in order to remove the adhesive excesses and the oxygen-inhibition layer.

We tested half of the sample 24 h after preparation and the other half 28 days after water storage at 37 °C. The cross-sectional area of each stick was measured with the digital caliper to the nearest 0.01 mm and recorded for subsequent calculation of the ultimate tensile strength values (Absolute Digimatic, Mitutoyo, Tokyo, Japan). It was attached each specimen to a modified device with cyanoacrylate resin (IC-Gel, bSi Inc., Atascadero, CA, USA) and subjected it to a tensile force at 0.5 mm/min. Five specimens were tested per group.

2.5. In vitro degree of conversion

One drop (10 μL) of the adhesive solution was individually placed between acetate strips to achieve a thin adhesive film of approximately 8 mm in diameter. Before covering the drops of adhesive with the upper acetate strip, they were gently air-dried with a dry stream (10 s at a distance of 10 cm) to allow solvent evaporation. After covering the drops of adhesive with the upper acetate strip, each specimen was photo-activated for 10 s at 1000 mW/cm^2 (VALO, Ultradent Products, South Jordan, UT, USA) and carefully removed from the acetate strip with a narrow surgical knife and stored for 24 h in a dark, dry environment until analysis.

A Fourier Transformed Infrared (FTIR; IRPrestige-21, Shimadzu, Tokyo, Japan) spectrum of the polymerized specimens and unpolymerized material was recorded. The spectrum was obtained with 32 scans at 1 cm^{-1} resolution by a transmission method. The percentage of unreacted carbon–carbon double bonds (%C=C) was determined from the ratio of absorbance intensities of aliphatic C=C (peak height at 1639 cm^{-1}) against an internal standard before and after specimen polymerization. The aromatic carbon–carbon bond (peak height at 1609 cm^{-1}) absorbance was used as an internal standard. The degree of conversion was determined by subtracting the %C=C from 100%. Three specimens were tested for each group.

2.6. Teeth preparation and bonding procedures

Eighty-four caries-free extracted human third molars, collected from patients with age ranging from 18 to 35 years old were used. The teeth were collected after the patient's informed consent. The University Ethics Committee approved this study under protocol number 2.399.496. Teeth were disinfected in 0.5% chloramine, stored in distilled water and used within 3 months after extraction. A flat dentin surface was exposed on each tooth after wet grinding the occlusal enamel with 180-grit SiC paper.

2.6.1. Microbiological caries induction

The external surface of each specimen was covered with one layer of epoxy resin (Araldite, Brascola Ltda, São Bernardo do Campo, Brazil) and one layer of nail varnish (Colorama Maybelline Ltda, São Paulo, Brazil) with the exception of the occlusal surface. The teeth were sterilized in steam autoclave (Phoenix Ind. Brasileira, Araraquara, SP, Brazil) for 15 min at 121 °C (Carvalho et al., 2009), and each tooth was individually immersed in an 8 mL falcon tube containing an artificial caries solution. The solution contained 9.25 g of brain heart infusion culture supplemented with 1.25 g of yeast extract, 5.0 g of sucrose, in 250 mL of distilled water and 100 μL of primary culture of *S. mutans* (ATCC 25175), with the pH around 4.0. The specimens were incubated in an anaerobic jar (5% CO_2) at 37 °C. At every 48 h, the specimens were transferred to another 8 mL falcon tube containing a new artificial caries solution. After 14 days, all the specimens were again sterilized as aforementioned and washed in deionized water (Marquezan et al., 2009).

2.6.2. Bonding procedures

Before the bonding procedures, the surrounding enamel of all teeth was grinding with a diamond bur nº 4137 (KG Sorensen, Barueri, São Paulo, Brazil), until the dentin surface was exposed. Then, the occlusal dentin surfaces were further polished with 600-grit silicon-carbide paper for 30 s to standardize the smear layer and simulated caries-affected dentin.

The adhesives were applied at etch-and rinse (ER) or self-etch (SE) mode, as per manufacturer' instructions (Table 2) (n = 7 in ER mode and n = 7 in SE mode, per group). In ER mode, the dentin surface was acid etched with 37% phosphoric acid for 15 s (Condac, FGM Prod. Odont. Ltda, Joinville, SC, Brazil), water rinsed for 15 s and dried with absorbent paper keeping the dentin surface slightly wet. After the bonding procedures, resin composite restorations (Opallis, FGM Prod. Odont. Ltda, Joinville, SC, Brazil) were buildup on the bonded surfaces in 3 increments of 1.0 mm thick each and each one was individually light activated for 40 s (VALO, Ultradent Products, South Jordan, UT, USA). A single operator carried out all bonding procedures in an environment with controlled temperature and humidity. Five teeth were used for each experimental group.

After storage of the bonded teeth in distilled water at 37 °C for 24 h, 24 teeth were longitudinally sectioned in "x" direction across the bonded interface with a diamond saw in a cutting machine (IsoMet 1000; Buehler, Lake Bluff, USA), under water cooling at 300 rpm to obtain resin-dentin slices with a thickness of approximately 1.2 mm^2 for nanoleakage and *in situ* degree of conversion test. On the other hand, 60 teeth were longitudinally sectioned in both "x" and "y" directions across the bonded interface to obtain resin-dentin sticks with a cross-sectional area of approximately 0.8 mm^2. The number of premature failures (PF) per tooth during specimen preparation was recorded. The cross-sectional area of each stick was measured with the digital caliper to the nearest 0.01 mm and recorded for subsequent calculation of the microtensile bond strength values (Absolute Digimatic, Mitutoyo, Tokyo, Japan).

Table 2
Universal adhesive system (batch number), composition [a] and application mode.

Universal adhesive system (batch number) and pH	Composition ([a])	Etch-and-rinse mode	Self-etch mode
Prime&Bond Active (PBA - Dentsply-Sirona, Konstanz, Baden-Württemberg, Germany) (1703000452) pH = ~2.5	Phosphoric acid modified acrylate resin, multifunctional acrylate, bifunctional acrylate, acidic acrylate, isopropanol, water, initiator, Stabilizer (10-MDP and PENTA)	1. Apply phosphoric acid for 15 s. 2. Remove gel with vigorous water spray and rinse conditioned areas thoroughly for 15 s. 3. Remove rinsing water completely by blowing gently with an air syringe or blot dry. Do not desiccate dentin. 4. Apply adhesive to completely wet the surfaces to be treated. If necessary rewet applicator tip. Avoid pooling of the adhesive. 5. Keep the adhesive slightly agitated for 20 s. 6. Disperse adhesive and remove solvent with clean, dry air from an air-water syringe. Treat every surface with a moderate air flow for at least 5 s until a glossy and uniform layer results. 7. Light cure for 10 s at 1200 mW/cm^2	1. Apply adhesive to completely wet the surfaces to be treated. If necessary rewet applicator tip. Avoid pooling of the adhesive. 2. Keep the adhesive slightly agitated for 20 s. 3. Disperse adhesive and remove solvent with clean, dry air from an air-water syringe. Treat every surface with a moderate air flow for at least 5 s until a glossy and uniform layer results. 4. Light cure for 10 s at 1200 mW/cm^2
Ambar Universal (AMU - FGM Prod. Odontológicos, Joinville, Santa Catarina, Brazil) (310516) pH = 2.6–3.0	10-MDP, methacrylic monomers, photoinitiators, coinitiators, stabilizers, silica nanoparticles and ethanol	1. Apply phosphoric acid for 15 s. 2. Wash the surface with plenty of water and dry the cavity so that the dentin does not get dehydrated, but without the accumulation of water on the surface. 3. Apply a first layer vigorously rubbing the adhesive with the micro applicator for 10 s. 4. Next, apply a second layer of adhesive for 10 s, spreading the product. 5. Evaporate excess solvent by thoroughly air-drying with an air syringe for 10 s 6. Light cure for 10 s at 1200 mW/cm^2	1. Apply a first layer vigorously rubbing the adhesive with the micro applicator for 10 s. 2. Next, apply a second layer of adhesive for 10 s, spreading the product. 3. Evaporate excess solvent by thoroughly air-drying with an air syringe for 10 s 4. Light cure for 10 s at 1200 mW/cm^2

[a] 10-MDP = methacryloyloxydecyl dihydrogen phosphate; PENTA = dipentaerythritol penta acrylate monophosphate.

2.7. Microtensile bond strength testing

Each stick was attached to a modified device for microtensile bond strength test with cyanoacrylate resin (IC-Gel, bSi Inc., Atascadero, CA, USA) and subjected to a tensile force in a universal testing machine (Kratos, São Paulo, SP, Brazil) at 0.5 mm/min. The failure mode was evaluated under an optical microscope (SZH-131, Olympus; Tokyo, Japan) at 40x and classified as cohesive in dentin (failure exclusive within cohesive dentin – CD); cohesive in resin (failure exclusive within cohesive resin – CR); adhesive (failure at resin/dentin interface – A), or mixed (failure at resin/dentin interface that included cohesive failure of the neighboring substrates, M). The number of premature failures (PF) was recorded and it was not included in the average mean bond strength.

2.8. Nanoleakage evaluation

Before performing the nanoleakage test a pilot test was conducted to evaluate if the presence of zinc and copper in the adhesive could impair the visualization of silver nitrate uptake. For this purpose, we performed scanning electron microscopy images of resin-dentin interfaces of all groups without immersion in silver nitrate. Even in adhesive interfaces with the highest zinc (5%) or copper (0.2%) concentration, ZnONp and CuNp were not observed using the same parameters described above. And thus, the results of nanoleakage test reflect the amount of silver uptake into unpolymerized areas and/or nanospaces not infiltrated by the resin adhesive but not the presence of zinc or copper in the hybrid layer.

After this preliminary test, all resin-dentin slices selected for this test were coated with two layers of nail varnish applied up to within 1 mm of the bonded interfaces. The resin-dentin slices were immersed in 50 wt% ammoniacal silver nitrate solution in total darkness for 24 h, rinsed thoroughly in distilled water, and immersed in photo developing solution for 8 h under a fluorescent light to reduce silver ions into metallic silver grains within voids along the bonded interface.

Specimens were mounted on aluminium stubs, polished with 1000-, 1500-, 2000- and 2500-grit SiC paper and 1 and 0.25 μm diamond paste (Buehler Ltd., Lake Bluff, IL, USA). Then, they were ultrasonically cleaned, air dried and gold sputter coated (MED 010, Balzers Union, Balzers, Liechtenstein). The interfaces were observed in a scanning electron microscope in the backscattered mode at 12 kV (VEGA 3 TESCAN, Shimadzu, Tokyo, Japan).

In a way to standardize image acquisition, five pictures were taken of each specimen. The first picture was taken in the center of the resin-dentin slice. The other four pictures were taken 0.3 and 0.6 mm to the left and right of the first one. The resin-dentin slices were evaluated and a total of two teeth were used for each experimental condition, a total of 10 images were evaluated per group. A technician who was blinded to the experimental conditions under evaluation took them all. The relative percentage of nanoleakage within the adhesive and hybrid layer areas was measured in all pictures using the public domain Image J software, a Java-based image processing software package developed at the National Institutes of Health (NIH) (Schneider et al., 2012).

2.9. In situ degree of conversion within adhesive/hybrid layers

All resin-dentin slices selected for this test were wet polished using 1500; 2000; 2500 and 4000-grit SiC paper for 30 s each. The specimens were ultrasonically cleaned for 10 min and positioned into micro-Raman equipment. The DC measurements were performed in a micro-Raman spectrometer (Bruker Optik GmbH, Ettlingen, Baden-Württemberg, Germany). The micro-Raman spectrometer was first calibrated for zero and then for coefficient values using a silicon specimen. Specimens were analyzed using the following micro-Raman parameters: 20-mW Neon laser with 532-nm wavelength, spectral resolution $\approx 1\ cm^{-1}$, accumulation time of 30 s with 6 co-additions, and magnification of 100x (Olympus UK, London, UK) to beam diameter of ≈ 1 μm (Hass et al., 2012, 2013; Perdigão et al., 2014). The spectra were taken at the resin-dentin interface, in the middle of the hybrid layer within the intertubular dentin, at five different sites for each specimen selected at line-scan mode and the values averaged for statistical purposes. Spectra of uncured adhesives were taken as reference. Post-processing of spectra was performed using the dedicated Opus Spectroscopy Software version 6.5 (Bruker Optik GmbH, Ettlingen, Baden-Württemberg, Germany).

The ratio of the double-bond content of monomer to polymer in the adhesive was calculated according to the following formula: DC (%) = $(1 - R_{cured}/R_{uncured})$ x 100, where R is the ratio of aliphatic and aromatic peak areas at $1639\ cm^{-1}$ and $1609\ cm^{-1}$ in cured and uncured adhesives.

2.10. Identification of copper within adhesive itself by EDX

Three adhesive discs of each group were produced as described for the microbiological test. After preparation, specimens were stored in a dark vial for 24 h and vertically sectioned in the middle with a diamond saw in a cutting machine (IsoMet 1000; Buehler, Lake Bluff, USA), under water cooling (at 300 rpm). Then, 4 areas of this cross-sectional interface were observed by field emission scanning electron microscope (FE-SEM) (MIRA 3 TESCAN, Shimadzu, Tokyo, Japan) coupled with an energy-dispersive X-ray spectrometer (EDX) in order to evaluate the uniform dispersion of ZnO/CuNp within the adhesive matrix (Gutierrez et al., 2017a).

2.11. Statistical analysis

The data were first analyzed using the Kolmogorov-Smirnov test to assess whether the data followed a normal distribution, as well as Barlett's test for equality of variances to determine if the assumption of equal variances was valid. After confirming the normality of the data distribution and the equality of the variances, data for MMP activity (RFU) and *in vitro* degree of conversion (%) of each adhesive were subjected to a one-way ANOVA. Data for microbiological test (mm), ultimate tensile strength (UTS), μTBS (MPa), nanoleakage (%) and *in situ* degree of conversion (%) of each adhesive were subjected to two-way ANOVA. Tukey's post hoc test was used for pair-wise comparisons ($\alpha = 0.05$) using the Statistica for Windows software (StatSoft, Tulsa, OK, USA).

3. Results

3.1. Anti-MMP activity

MMP-2 activity levels were significantly lower for 5/0.1 and 5/0.2 groups when compared with positive controls, showing inhibitory activity ($p < 0.01$). No significant differences among 5/0.1 and 5/0.2 groups and inhibitor control were detected ($p > 0.05$) (Fig. 1).

MMP-8 activity levels for the 5/0.2 group were significantly lower when compared with positive controls, showing inhibitory activity ($p < 0.01$). The 5/0.1 group did not show significant inhibitory activity ($p > 0.05$). Similarly, no significant differences among 5/0.1 and 5/0.2 groups and inhibitor control were detected ($p > 0.05$) (Fig. 1).

Finally, MMP-9 activity levels were significantly lower for 5/0.1 and 5/0.2 groups when compared with positive controls, showing inhibitory activity ($p < 0.01$). The 5/0.1 group showed significantly higher activity levels when compared with the inhibitor control and 5/0.2 groups ($p < 0.05$) (Fig. 1).

3.2. Antimicrobial activity

The results of antimicrobial activity against *S. mutans* for the different concentrations of ZnO/CuNp, incorporated in universal

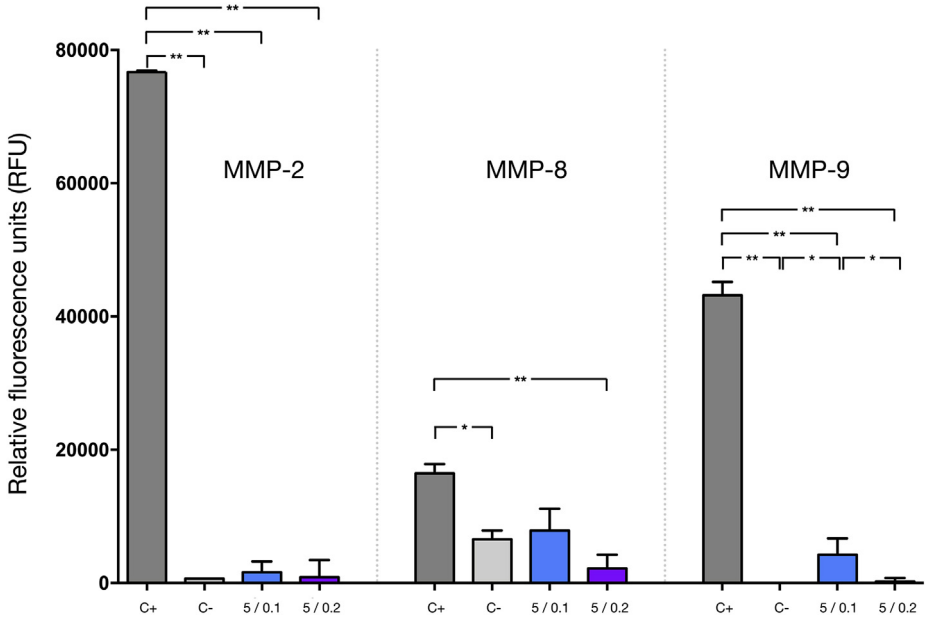

Fig. 1. Assay results for matrix metalloprotease (MMP)–2, MMP-8 and MMP-9 inhibition by zinc oxide and copper nanoparticles (ZnO/CuNp). Diluted active MMP as positive controls (C+), 25 μM Ilomastat as inhibitor control (C-). *$P < 0.05$; **$P < 0.01$.

Table 3
Means and standard deviations of bacterial inhibition halo sizes (mm) against *S. mutans,* obtained in each experimental condition [a].

ZnO/Cu concentration (%)	Prime&Bond Active		Ambar Universal	
	Non-polymerized	Polymerized	Non-polymerized	Polymerized
0 (control)	9.2 ± 0.9 b	6.7 ± 0.5 c	8.1 ± 0.3 B	5.7 ± 0.4 C
5/0.1	12.9 ± 0.6 a	7.9 ± 0.7 b,c	11.1 ± 1.2 A	6.7 ± 0.8 B,C
5/0.2	13.0 ± 1.0 a	8.8 ± 0.9 b	12.0 ± 1.0 A	7.6 ± 0.6 B

[a] Comparisons are valid only for each adhesive. Means identified with the same capital, lowercase or uppercase letters are statistically similar. (Tukey's test, $p \geq 0.05$).

adhesives systems, are shown in Table 3. When the both adhesives were non-polymerized, all ZnO/Cu-containing solutions showed significantly higher antibacterial properties against *S. mutans* significantly higher than controls ($p < 0.01$). On the other hand, when the both adhesives were polymerized, only the 5/0.2 groups showed significantly higher antibacterial properties against *S. mutans* significantly higher than respective controls ($p < 0.05$).

3.3. Ultimate tensile strength

When the ZnO/CuNp were incorporated into the Prime&Bond Active adhesive, no significant differences among ZnO/CuNp groups and control were observed, after 24 h or after 28-days (Table 4; $p > 0.05$). A significant decrease in the ultimate tensile strength after 28-days of water storage was observed in all groups (Table 4; $p < 0.001$).

For Ambar Universal adhesive, groups with ZnO/CuNp showed higher ultimate tensile strength values than control, after 24 h and 28-days (Table 4; $p < 0.001$) and no significant differences in the ultimate tensile strength after 28-days of water storage was observed in all groups (Table 4; $p > 0.05$).

3.4. In vitro degree of conversion

For *in vitro* degree of conversion, no significant differences among groups were detected when the ZnO/CuNp were incorporated into the Prime&Bond Active (Table 4; $p = 0.20$) and Ambar Universal adhesives (Table 4; $p = 0.84$).

Table 4
Means and standard deviations of the 24 h and 28-days ultimate tensile strength (UTS, MPa) and degree of conversion (DC, %) obtained in each experimental condition [a].

ZnO/Cu concentration (%)	Prime&Bond Active			Ambar Universal		
	24 h UTS	28-days UTS	*in vitro* DC	24 h UTS	28-days UTS	*in vitro* DC
0 (control)	5.97 ± 0.32 ^{A}	3.35 ± 0.34 ^{B}	52.33 ± 1.04 $_{a}$	17.20 ± 1.67 A	17.00 ± 1.54 A	67.69 ± 3.70 ^{a}
5/0.1	5.77 ± 0.79 ^{A}	3.57 ± 0.40 ^{B}	54.59 ± 1.50 $_{a}$	23.85 ± 1.01 B	22.94 ± 1.76 B	68.86 ± 2.09 ^{a}
5/0.2	6.97 ± 1.38 ^{A}	3.60 ± 0.66 ^{B}	55.17 ± 2.44 $_{a}$	24.00 ± 0.94 B	23.85 ± 1.68 B	68.58 ± 0.92 ^{a}

[a]Comparisons are valid only within adhesive and test. Means identified with the same capital or lowercase letter, subscript or not subscripted letters are statistically similar. (Tukey's test, $p \geq 0.05$).

Table 5
Means and standard deviations of microtensile bond strength (MPa) obtained in each experimental condition[a].

ZnO/Cu concentration (%)	Prime&Bond Active		Ambar Universal	
	Etch-and-rinse	Self-etch	Etch-and-rinse	Self-etch
0 (control)	27.7 ± 5.9 A	30.6 ± 3.4 A	30.3 ± 2.54 a	18.9 ± 6.3 b
5/0.1	28.3 ± 5.3 A	29.0 ± 6.4 A	30.1 ± 5.45 a	24.4 ± 3.4 a,b
5/0.2	27.2 ± 5.0 A	30.7 ± 4.3 A	33.6 ± 5.52 a	24.9 ± 2.8 a,b

[a] Comparisons are valid only within adhesive. Means identified with the same capital or lowercase letter are statistically similar. (Tukey's test, p ≥ 0.05).

3.5. Microtensile bond strength testing

For Prime&Bond Active, no significant differences were observed in the microtensile bond strength among all groups, in both adhesive strategies (Table 5; $p > 0.05$). For Ambar Universal, no significant differences were observed in the microtensile bond strength among all groups, when ZnO/CuNp were added (Table 5; $p > 0.05$). A significant difference between adhesive strategies was observed only in control group (Table 5; $p < 0.05$).

3.6. Nanoleakage evaluation of resin-dentin interfaces

For Prime&Bond Active and Ambar Universal, it was observed that the addition of ZnO/CuNp showed lower nanoleakage values than control, in both adhesive strategies (Table 6 and Fig. 2; $p < 0.05$). A significant difference between adhesive strategies was observed for Ambar Universal only in control group (Table 6 and Fig. 2; $p < 0.001$).

3.7. In situ degree of conversion within adhesive/hybrid layers

For Prime&Bond Active and Ambar Universal, no significant differences were observed for *in situ* degree of conversion among all groups, in either of the adhesive strategies (Table 7; $p > 0.05$). No differences were showed between adhesive strategies in all groups, in both adhesive system (Table 7; $p > 0.05$).

3.8. Identification of zinc oxide and copper within adhesive itself by EDX

Representative EDX spectrum of the adhesive specimens with 5/0.1 wt% ZnO/CuNp (Fig. 3) shows the presence of zinc oxide and copper in the surface and underneath the adhesive. The same pattern was observed for all ZnO/CuNp-containing universal adhesives (data not shown).

4. Discussion

The idea behind the incorporation of ZnONp and CuNp into adhesive formulations was to add antimicrobial properties. Several studies have shown the antimicrobial properties of ZnONp (Hernandez-Sierra et al., 2008) and CuNp (Amiri et al., 2017) when evaluated alone, or when dental adhesives were doped with ZnONp (Saffarpour et al., 2016) or CuNp (Gutierrez et al., 2017a, 2017b), but there is not much evidence about the antimicrobial effects of combination of both nanoparticles. A recent study showed antibacterial effects of the combination of zinc and copper nanoparticles in aqueous solution against *Staphylococcus aureus* (Wang et al., 2016), however to extent of our knowledge, this is the first study that observe an antibacterial effect when both nanoparticles were added together in a dental adhesive.

In the current study it was observed that, when the adhesives were non-polymerized, all ZnO/Cu-containing solutions showed antibacterial properties against *S. mutans* significantly higher than control. On the other side, only 5/0.2 ZnO/CuNp groups showed antibacterial properties significantly higher than respective control when the adhesives were polymerized.

The higher antibacterial properties against *S. mutans* of 5/0.2 groups than respective control can be explained because ZnONp and, particularly in this case, CuNp have an antibacterial activity that is size- and concentration-dependent (Azam et al., 2012; Padmavathy and Vijayaraghavan, 2008; Pandiyarajan et al., 2013). As it was increasing the concentration of CuNp twice, it may be that copper metal ions can diffuse, and eventually, entrain zinc oxide metal ions, despite the thin layer of adhesive present in the filter disc.

Several mechanisms have been proposed by which the ZnONp and CuNp could exert their antimicrobial effect (Dizaj et al., 2014; Palza, 2015; Sabella et al., 2014). A more recent theory is called “Trojan horse effect”, where due to endocytosis processes, the acidic lysosomal environment (pH 5.5) is capable of promoting catalyzed radical formation and nanoparticles degradation/corrosion, which converts core metals to ions and therefore toxic substances (Sabella et al., 2014). Nevertheless, the possible synergistic antibacterial mechanisms of the multicomponent metal ions-containing require further investigations. It worth to mention that, although the antibacterial properties of both adhesives in the 5/0.2 ZnO/CuNp groups, it was showed in a previously study that, in this concentration the adhesive was not highly cytotoxic (Gutierrez et al., 2019).

Recent studies have shown that the incorporation of ZnONp (Garcia et al., 2016) and CuNp (Gutierrez et al., 2017b) into dental adhesives not influence negatively the ultimate tensile strength. In the current study, agreeing with these results, when the ZnO/CuNp were incorporated into the Prime&Bond Active adhesive, we can observe that no significant differences among ZnO/CuNp groups and control were observed, after 24 h and after 28-days. However, a significant decrease in UTS values after 28-days of water storage was observed in all groups. This could be explained by the presence of dipentaerythritol penta acrylate monophosphate (PENTA), a very hydrophilic resin monomer which contribute to a higher water sorption (Gutierrez et al., 2019), what could counteract the catalytic effect of copper, explaining why the addition of ZnO/CuNp does not improve the UTS values after 24 h and after 28d. In addition to that, the addition of 5/0.1 and 5/0.2 ZnO/CuNp increased the solubility of the Prime&Bond Active adhesive (Gutierrez et al., 2019) by the presence of isopropanol, a highly water-soluble solvent (NCBI, 2018 in the adhesive composition (Dentsply Sirona, 2017), what along with the greatest water sorption makes the material more prone to early degradation and affecting negatively the resistance UTS values after 28d in all groups. On the other hand, when the ZnO/CuNp were incorporated into the Ambar Universal adhesive,

Table 6
Means and standard deviations of nanoleakage (%) obtained in each experimental condition[a].

ZnO/Cu concentration (%)	Prime&Bond Active		Ambar Universal	
	Etch-and-rinse	Self-etch	Etch-and-rinse	Self-etch
0 (control)	13.1 ± 2.7 A	14.0 ± 2.7 A	13.2 ± 4.1 a	7.2 ± 2.7 b
5/0.1	8.1 ± 1.6 B	8.5 ± 1.4 B	4.0 ± 1.3 b,c	3.2 ± 1.1 c
5/0.2	7.3 ± 1.8 B	7.3 ± 1.6 B	3.4 ± 1.3 c	3.0 ± 0.6 c

[a] Comparisons are valid only within adhesive. Means identified with the same capital or lowercase letter are statistically similar. (Tukey's test, p ≥ 0.05).

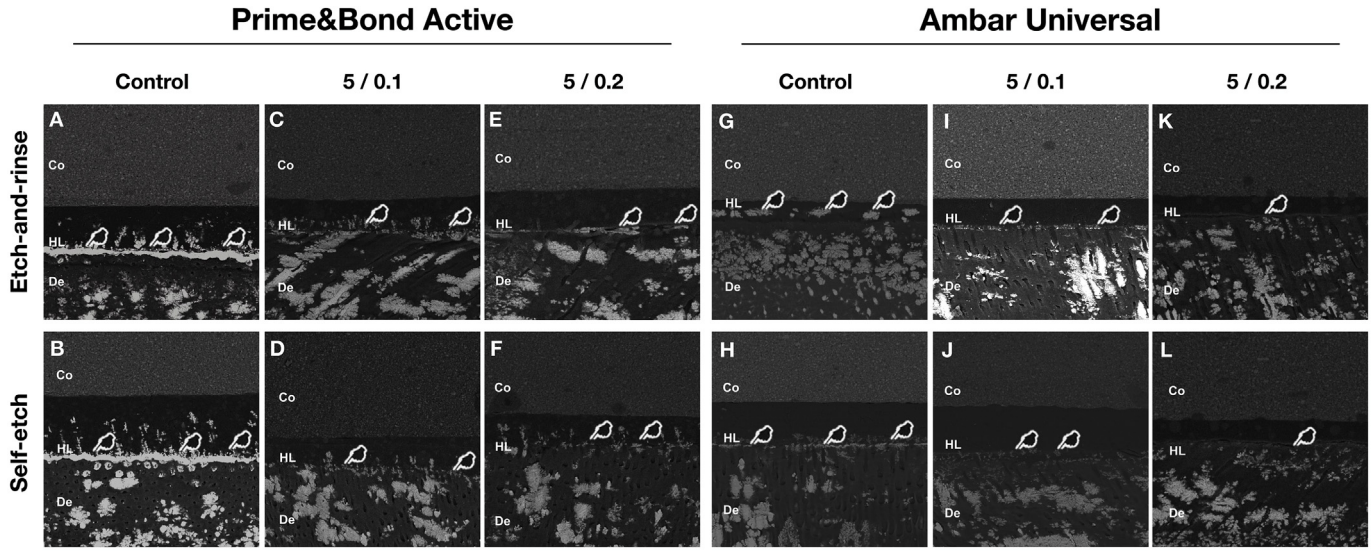

Fig. 2. Representative back-scattering SEM images of the resin–caries-affected dentin interfaces according to the different experimental conditions. In the ZnO/CuNp-containing adhesive groups (C–F for Prime&Bond Active and I-L for Ambar Universal) we can see lower silver nitrate deposition than the control groups (A-B for Prime&Bond Active and G-H for Ambar Universal) (white stains indicated by white pointer). (Co = composite; HL = hybrid layer and De = dentin).

Table 7
Means and standard deviations of the *in situ* degree of conversion within adhesive/hybrid layer (%) obtained in each experimental condition[a].

ZnO/Cu concentration (%)	Prime&Bond Active		Ambar Universal	
	Etch-and-rinse	Self-etch	Etch-and-rinse	Self-etch
0 (control)	54.5 ± 2.9 A	53.4 ± 3.8 A	63.4 ± 1.3 a	62.4 ± 2.2 a
5/0.1	55.0 ± 0.8 A	55.5 ± 1.8 A	65.9 ± 2.7 a	63.6 ± 3.6 a
5/0.2	54.5 ± 2.6 A	55.4 ± 7.2 A	65.2 ± 4.5 a	65.3 ± 2.1 a

[a] Comparisons are valid only within adhesive. Means identified with the same capital or lowercase letter are statistically similar. (Tukey's test, $p \geq 0.05$).

groups with ZnO/CuNp showed higher ultimate tensile strength values than control, after 24 h and 28-days. This could be explained for the catalytic effect of copper, that form a tough and low stress homogeneous glassy crosslinked network in the adhesive (Song et al., 2016).

On the other hand, several studies have demonstrated the MMP inhibitory properties of zinc (Osorio et al., 2011) and copper (Jun et al., 2018), but no study had previously demonstrated the MMP inhibitory potential of the combination of both ions. In the current study it was demonstrated that the combination of ZnONp and CuNp inhibits MMP-2, MMP-8 and MMP-9, proteolytically active during the carious process (Mazzoni et al., 2015), what would help maintain the stability of the interface to caries-affected dentin interface over time. In this sense, for both universal adhesive systems, all ZnO/CuNp groups showed similar values of resin-caries-affected dentin bond strength than control, which

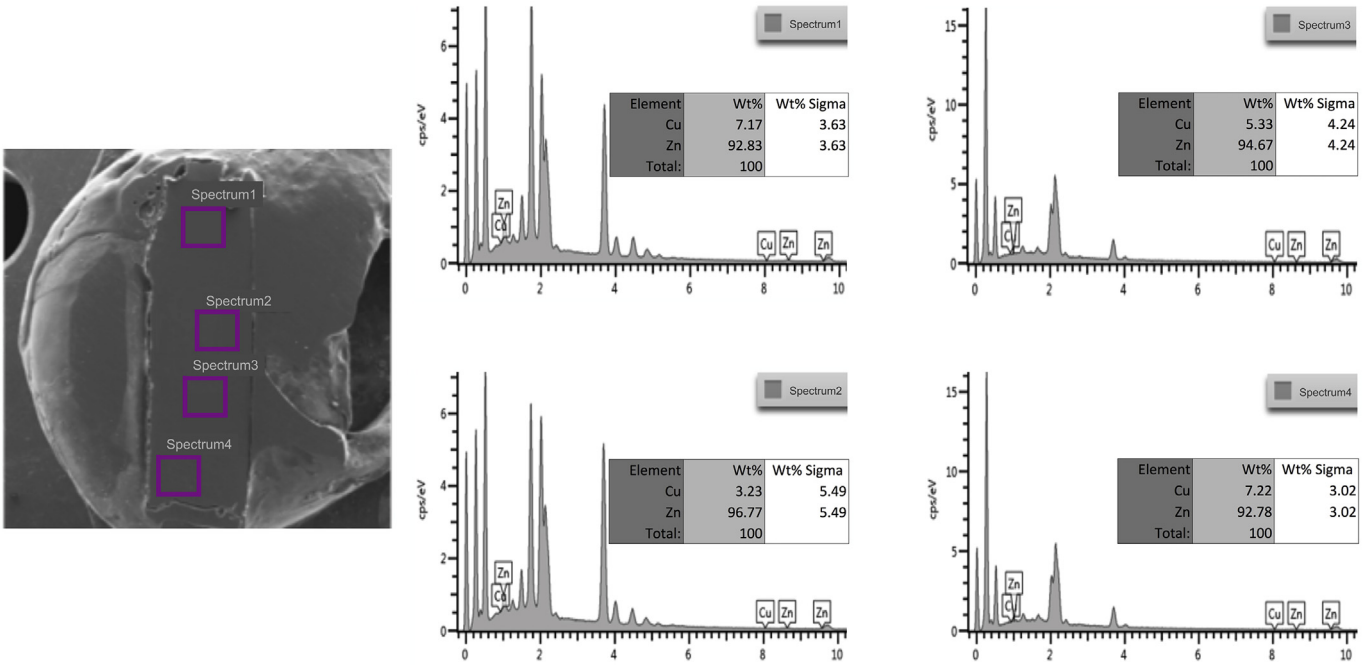

Fig. 3. EDX spectrum of the body of a representative adhesive specimen with 5/0.1 wt% ZnO/CuNp. EDX spectra from different selected area of the adhesive body outlined by a magenta rectangle in. The figure table summarizes the elemental composition of the sample area outlined.

agrees with a recent systematic review and meta-analysis, which mentions that the use of MMP inhibitors did not affect the immediate bond strength, while it influenced the aged bond strength. Therefore, studies that evaluate resin-caries-affected dentin bond strength over time are necessary. When all adhesives were used in etch-and-rinse application mode, values between 27.2 and 33.6 MPa were observed (27.2–27.7 for PBA and 30.1–33.6 for AMB), whereas when they were used in self-etch application mode, values between 18.9 and 30.7 MPa (29.0–30.7 for PBA and 18.9–24.9 for AMB) were observed. These results are consistent with previous studies realized on caries-affected dentin, when the adhesives were used in the etch-and-rinse or self-etch strategy (Isolan et al., 2018).

More interesting were the nanoleakage and microleakage results. These tests reveal the location of defects at the resin-dentin interface that may serve as pathways for degradation of resin-dentin bonds over time. Silver nitrate ions used to trace nanoleakage or fluorescein sodium salt used for microleakage, occupy spaces around unprotected collagen fibrils, where resin failed to infiltrate or where residual water/solvent were not displaced by the adhesive resin. In the current study it was observed that for both adhesives, independently of the application mode, there was a significant decrease in nanoleakage. This could be explained because copper can increase the strength of the collagen network, one of the components of the hybrid layer, because the collagen cross-linking enzyme, lysyl oxidase (LOX), is copper dependent (Marelli et al., 2015; Rucker et al., 1998) and thus copper has an indirect effect as a cross-linking agent. Other study showed that, the incorporation of ZnO has resulted in the formation of apatite crystallites on the collagen fibrils, favoring dentin mineralization (Toledano et al., 2013) and improved the cross-linking effect. This cross-linker action of both nanoparticles may increase the resistance of collagen, leaving it less susceptible to the effects of proteolytic enzymes, indirectly decreasing the immediate nanoleakage, as well as previously showed by adhesive-containing CuNp (Gutierrez et al., 2017a, 2017b) and ZnO alone (Toledano et al., 2017).

Because the characteristics of caries-affected dentin, like altered cross-striated pattern of organic matrix of the collagen fibrils and non-collagenous proteins, and an increased porosity (Tjäderhane et al., 2015), resulting in increased dentin humidity and significantly reduced dentin mechanical properties (Ito et al., 2005; Tjäderhane, 2019), in addition to the characteristics of universal adhesives, which are ultimately simplified adhesives that act as permeable membranes to dentinal moisture, adhesive restorations on caries-affected dentin is challenging for clinicians, what makes essential and vitally important the development of materials with antibacterial, enzymatic inhibitors and cross-linker properties, in order to increase the durability of the adhesive/caries-affected dentin interface, without compromising the mechanical properties of the adhesive (Cocco et al., 2015).

Recent studies have shown that the incorporation of ZnONp (Garcia et al., 2016) or CuNp (Gutierrez et al., 2017a, 2017b) into dental adhesives not influence negatively the mechanical properties of the adhesive itself, as well as, observed in the ultimate tensile strength results of the present study. However, a significant decrease in mechanical properties values after 28-days of water storage was observed in all groups for Prime&Bond Active adhesive. It can be explained by the presence of dipentaerythritol penta acrylate monophosphate (PENTA), a highly hydrophilic resin monomer which contribute to a higher water sorption (Gutierrez et al., 2019), making the material more prone to early degradation and affecting negatively the resistance ultimate tensile strength values. On the other hand, when the ZnO/CuNp were incorporated into the Ambar Universal adhesive, groups with ZnO/CuNp showed higher ultimate tensile strength values than control, after 24 h and 28-days. This could be explained for the catalytic effect of copper, that form a tough and low stress homogeneous glassy crosslinked network in the adhesive (Song et al., 2016). In addition, for both adhesive systems, the incorporation of ZnO/CuNp not negatively influenced the *in vitro* and *in situ* degree of conversion. The similar degree of conversion of the experimental groups compared to control is probably due to the fact that ZnONp and CuNp shown to have a good compatibility with chemicals when added to methacrylate polymer and adhesives systems.

As limitations of this study, we can mention that, although the results of the present study showed significant increases in antimicrobial activity against *S. mutans*, it is not clear whether this difference is clinically relevant. In addition, the results of the current study do not demonstrate a broad-spectrum antibacterial effect, just as we cannot mention these results as a definitive solution to the process that causes secondary caries. Moreover, the limitations of caries microbiological induction models in their desire to simulate caries-affected dentin that we observe clinically are well known. However, we believe that the addition of antimicrobial properties to adhesive systems could be an alternative to avoid the appearance of secondary caries, understanding that it is a complex and multifactorial process, being an important step in the search for solutions to the process mentioned above. In this context, new studies that improve the previously existing models of artificial caries induction, as well as long term studies in order to corroborate the antibacterial and anti-MMP properties, verifying the clinical relevance of these results.

Thus, the present study was capable to demonstrate that the addition of zinc oxide and copper nanoparticles to two universal adhesive systems could provide them antimicrobial activity against *S. mutans* and anti-MMP properties, without negative influence on the mechanical properties, improving the quality of resin/caries-affected dentin interface.

5. Conclusions

The addition of zinc oxide and copper nanoparticles in concentrations up to 5/0.2 wt% in two universal adhesive systems is a feasible approach and may be an alternative to adhesive interfaces with antimicrobial activity against *S. mutans* and improves the integrity of the hybrid layer on caries-affected dentin.

Conflicts of interest

The authors declare no competing financial interest.

Acknowledgment

This study was performed by Mario Felipe Gutiérrez Reyes as partial fulfillment of his PhD degree at the State University of Ponta Grossa (UEPG), Ponta Grossa, PR, Brazil. This project was supported by Fondecyt (Fondo Nacional de Desarrollo Científico y Tecnológico - Chile) project 1170575 (Chile; EF). Also, this study was partially supported by the National Council for Scientific and Technological Development (CNPq) under grants 305588/2014-1 (Brazil; ADL) and in part by the Coordenação de Aperfeiçoamento de Pessoal de Nível Superior - Brasil (CAPES) - Finance Code 001.

Appendix A. Supplementary data

Supplementary data to this article can be found online at https://doi.org/10.1016/j.jmbbm.2019.07.024.

References

Amiri, M., Etemadifar, Z., Daneshkazemi, A., Nateghi, M., 2017. Antimicrobial effect of copper oxide nanoparticles on some oral bacteria and Candida species. J Dent Biomater 4, 347–352.

Azam, A., Ahmed, A.S., Oves, M., Khan, M.S., Memic, A., 2012. Size-dependent antimicrobial properties of CuO nanoparticles against Gram-positive and -negative bacterial strains. Int. J. Nanomed. 7, 3527–3535.

Barcellos, D.C., Fonseca, B.M., Pucci, C.R., Cavalcanti, B., Persici Ede, S., Goncalves, S.E., 2016. Zn-doped etch-and-rinse model dentin adhesives: dentin bond integrity,

biocompatibility, and properties. Dent. Mater. 32, 940–950.
Carvalho, F.G., Goncalves, L.S., Carlo, H.L., Soares, C.J., Correr-Sobrinho, L., Puppin-Rontani, R.M., 2009. Influence of sterilization method on the bond strength of caries-affected dentin. Braz. Oral Res. 23, 11–16.
Chaussain-Miller, C., Fioretti, F., Goldberg, M., Menashi, S., 2006. The role of matrix metalloproteinases (MMPs) in human caries. J. Dent. Res. 85, 22–32.
Cocco, A.R., Rosa, W.L., Silva, A.F., Lund, R.G., Piva, E., 2015. A systematic review about antibacterial monomers used in dental adhesive systems: current status and further prospects. Dent. Mater. 31, 1345–1362.
de Almeida Neves, A., Coutinho, E., Cardoso, M.V., Lambrechts, P., Van Meerbeek, B., 2011. Current concepts and techniques for caries excavation and adhesion to residual dentin. J. Adhesive Dent. 13, 7–22.
de Souza, A.P., Gerlach, R.F., Line, S.R., 2000. Inhibition of human gingival gelatinases (MMP-2 and MMP-9) by metal salts. Dent. Mater. 16, 103–108.
Dentsply Sirona, 2017. Dentsply Sirona FAQs. Accessed July 20 2017. https://www.dentsplysirona.com/content/dam/dentsply/pim/manufacturer/Restorative/Direct_Restoration/Adhesives/Universal_Adhesives/PrimeBond_active/PrimeBond%20active_Scientific%20Compendium_EN.pdf.
Dizaj, S.M., Lotfipour, F., Barzegar-Jalali, M., Zarrintan, M.H., Adibkia, K., 2014. Antimicrobial activity of the metals and metal oxide nanoparticles. Mater. Sci. Eng. C Mater. Biol. Appl. 44, 278–284.
FDI, 2017. Policy statement on minimal intervention dentistry (MID) for managing dental caries: adopted by the general assembly: september 2016, poznan, Poland. Int. Dent. J. 67, 6–7.
Garcia, I.M., Leitune, V.C., Kist, T.L., Takimi, A., Samuel, S.M., Collares, F.M., 2016. Quantum dots as nonagglomerated nanofillers for adhesive resins. J. Dent. Res. 95, 1401–1407.
Gregson, K.S., Shih, H., Gregory, R.L., 2012. The impact of three strains of oral bacteria on the surface and mechanical properties of a dental resin material. Clin. Oral Investig. 16, 1095–1103.
Gutierrez, M.F., Malaquias, P., Hass, V., Matos, T.P., Lourenco, L., Reis, A., Loguercio, A.D., Farago, P.V., 2017a. The role of copper nanoparticles in an etch-and-rinse adhesive on antimicrobial activity, mechanical properties and the durability of resin-dentine interfaces. J. Dent. 61, 12–20.
Gutierrez, M.F., Malaquias, P., Matos, T.P., Szesz, A., Souza, S., Bermudez, J., Reis, A., Loguercio, A.D., Farago, P.V., 2017b. Mechanical and microbiological properties and drug release modeling of an etch-and-rinse adhesive containing copper nanoparticles. Dent. Mater. 33, 309–320.
Gutierrez, M.F., Alegria-Acevedo, L.F., Mendez-Bauer, L., Bermudez, J., Davila-Sanchez, A., Buvinic, S., Hernandez-Moya, N., Reis, A., Loguercio, A.D., Farago, P.V., Martin, J., Fernandez, E., 2019. Biological, mechanical and adhesive properties of universal adhesives containing zinc and copper nanoparticles. J. Dent. 82, 45–55.
Hashimoto, M., Sasaki, J.I., Yamaguchi, S., Kawai, K., Kawakami, H., Iwasaki, Y., Imazato, S., 2015. Gold nanoparticles inhibit matrix metalloproteases without cytotoxicity. J. Dent. Res. 94, 1085–1091.
Hass, V., Luque-Martinez, I., Sabino, N.B., Loguercio, A.D., Reis, A., 2012. Prolonged exposure times of one-step self-etch adhesives on adhesive properties and durability of dentine bonds. J. Dent. 40, 1090–1102.
Hass, V., Dobrovolski, M., Zander-Grande, C., Martins, G.C., Gordillo, L.A., Rodrigues Accorinte Mde, L., Gomes, O.M., Loguercio, A.D., Reis, A., 2013. Correlation between degree of conversion, resin-dentin bond strength and nanoleakage of simplified etch-and-rinse adhesives. Dent. Mater. 29, 921–928.
Hebling, J., Pashley, D.H., Tjaderhane, L., Tay, F.R., 2005. Chlorhexidine arrests subclinical degradation of dentin hybrid layers in vivo. J. Dent. Res. 84, 741–746.
Hernandez-Sierra, J.F., Ruiz, F., Pena, D.C., Martinez-Gutierrez, F., Martinez, A.E., Guillen Ade, J., Tapia-Perez, H., Castanon, G.M., 2008. The antimicrobial sensitivity of Streptococcus mutans to nanoparticles of silver, zinc oxide, and gold. Nanomedicine 4, 237–240.
Huang, R., Li, M., Gregory, R.L., 2012. Effect of nicotine on growth and metabolism of Streptococcus mutans. Eur. J. Oral Sci. 120, 319–325.
Isolan, C.P., Sarkis-Onofre, R., Lima, G.S., Moraes, R.R., 2018. Bonding to sound and caries-affected dentin: a systematic review and meta-analysis. J. Adhesive Dent. 20, 7–18.
Ito, S., Saito, T., Tay, F.R., Carvalho, R.M., Yoshiyama, M., Pashley, D.H., 2005. Water content and apparent stiffness of non-caries versus caries-affected human dentin. J. Biomed. Mater. Res. B Appl. Biomater. 72, 109–116.
Jun, S.K., Yang, S.A., Kim, Y.J., El-Fiqi, A., Mandakhbayar, N., Kim, D.S., Roh, J., Sauro, S., Kim, H.W., Lee, J.H., Lee, H.H., 2018. Multi-functional nano-adhesive releasing therapeutic ions for MMP-deactivation and remineralization. Sci. Rep. 8, 5663.
Lynch, R.J., Churchley, D., Butler, A., Kearns, S., Thomas, G.V., Badrock, T.C., Cooper, L., Higham, S.M., 2011. Effects of zinc and fluoride on the remineralisation of artificial carious lesions under simulated plaque fluid conditions. Caries Res. 45, 313–322.
Marangos, O., Misra, A., Spencer, P., Bohaty, B., Katz, J.L., 2009. Physico-mechanical properties determination using microscale homotopic measurements: application to sound and caries-affected primary tooth dentin. Acta Biomater. 5, 1338–1348.
Marelli, B., Le Nihouannen, D., Hacking, S.A., Tran, S., Li, J., Murshed, M., Doillon, C.J., Ghezzi, C.E., Zhang, Y.L., Nazhat, S.N., Barralet, J.E., 2015. Newly identified inter-fibrillar collagen crosslinking suppresses cell proliferation and remodelling. Biomaterials 54, 126–135.
Marquezan, M., Correa, F.N., Sanabe, M.E., Rodrigues Filho, L.E., Hebling, J., Guedes-Pinto, A.C., Mendes, F.M., 2009. Artificial methods of dentine caries induction: a hardness and morphological comparative study. Arch. Oral Biol. 54, 1111–1117.
Mazzoni, A., Tjaderhane, L., Checchi, V., Di Lenarda, R., Salo, T., Tay, F.R., Pashley, D.H., Breschi, L., 2015. Role of dentin MMPs in caries progression and bond stability. J. Dent. Res. 94, 241–251.
NCBI, 2018. National Center for Biotechnology Information. CID = 3776. https://pubchem.ncbi.nlm.nih.gov/compound/3776 (accessed Aug. 15, 2018). PubChem Compound Database.
Orrego, S., Xu, H., Arola, D., 2017. Degradation in the fatigue crack growth resistance of human dentin by lactic acid. Mater. Sci. Eng. C Mater. Biol. Appl. 73, 716–725.
Osorio, R., Yamauti, M., Osorio, E., Ruiz-Requena, M.E., Pashley, D.H., Tay, F.R., Toledano, M., 2011. Zinc reduces collagen degradation in demineralized human dentin explants. J. Dent. 39, 148–153.
Padmavathy, N., Vijayaraghavan, R., 2008. Enhanced bioactivity of ZnO nanoparticles-an antimicrobial study. Sci. Technol. Adv. Mater. 9, 035004.
Palza, H., 2015. Antimicrobial polymers with metal nanoparticles. Int. J. Mol. Sci. 16, 2099–2116.
Pandiyarajan, T., Udayabhaskar, R., Vignesh, S., James, R.A., Karthikeyan, B., 2013. Synthesis and concentration dependent antibacterial activities of CuO nanoflakes. Mater. Sci. Eng. C Mater. Biol. Appl. 33, 2020–2024.
Perdigão, J., Munoz, M.A., Sezinando, A., Luque-Martinez, I.V., Staichak, R., Reis, A., Loguercio, A.D., 2014. Immediate adhesive properties to dentin and enamel of a universal adhesive associated with a hydrophobic resin coat. Oper. Dent. 39, 489–499.
Rucker, R.B., Kosonen, T., Clegg, M.S., Mitchell, A.E., Rucker, B.R., Uriu-Hare, J.Y., Keen, C.L., 1998. Copper, lysyl oxidase, and extracellular matrix protein cross-linking. Am. J. Clin. Nutr. 67, 996s–1002s.
Sabella, S., Carney, R.P., Brunetti, V., Malvindi, M.A., Al-Juffali, N., Vecchio, G., Janes, S.M., Bakr, O.M., Cingolani, R., Stellacci, F., Pompa, P.P., 2014. A general mechanism for intracellular toxicity of metal-containing nanoparticles. Nanoscale 6, 7052–7061.
Saffarpour, M., Rahmani, M., Tahriri, M., Peymani, A., 2016. Antimicrobial and bond strength properties of a dental adhesive containing zinc oxide nanoparticles. Braz. J. Oral Sci. 15, 66–69.
Schneider, C.A., Rasband, W.S., Eliceiri, K.W., 2012. NIH Image to ImageJ: 25 years of image analysis. Nat. Methods 9, 671–675.
Schrand, A.M., Rahman, M.F., Hussain, S.M., Schlager, J.J., Smith, D.A., Syed, A.F., 2010. Metal-based Nanoparticles and Their Toxicity Assessment. vol. 2. Wiley Interdiscip Rev Nanomed Nanobiotechnol., pp. 544–568.
Selwitz, R.H., Ismail, A.I., Pitts, N.B., 2007. Dental caries. Lancet 369, 51–59.
Song, H.B., Sowan, N., Shah, P.K., Baranek, A., Flores, A., Stansbury, J.W., Bowman, C.N., 2016. Reduced shrinkage stress via photo-initiated copper(I)-catalyzed cycloaddition polymerizations of azide-alkyne resins. Dent. Mater. 32, 1332–1342.
Takatsuka, T., Tanaka, K., Iijima, Y., 2005. Inhibition of dentine demineralization by zinc oxide: in vitro and in situ studies. Dent. Mater. 21, 1170–1177.
Tjäderhane, L., 2019. Dentin basic structure, composition, and function. In: Versiani, M., Basrani, B., Sousa-Neto, M. (Eds.), The Root Canal Anatomy in Permanent Dentition. Springer, Cham, Switzerland, pp. 17–27.
Tjäderhane, L., Buzalaf, M.A., Carrilho, M., Chaussain, C., 2015. Matrix metalloproteinases and other matrix proteinases in relation to cariology: the era of 'dentin degradomics. Caries Res. 49, 193–208.
Toledano, M., Nieto-Aguilar, R., Osorio, R., Campos, A., Osorio, E., Tay, F.R., Alaminos, M., 2010. Differential expression of matrix metalloproteinase-2 in human coronal and radicular sound and carious dentine. J. Dent. 38, 635–640.
Toledano, M., Yamauti, M., Ruiz-Requena, M.E., Osorio, R., 2012. A ZnO-doped adhesive reduced collagen degradation favouring dentine remineralization. J. Dent. 40, 756–765.
Toledano, M., Sauro, S., Cabello, I., Watson, T., Osorio, R., 2013. A Zn-doped etch-and-rinse adhesive may improve the mechanical properties and the integrity at the bonded-dentin interface. Dent. Mater. 29, e142–152.
Toledano, M., Osorio, R., Osorio, E., Cabello, I., Toledano-Osorio, M., Aguilera, F.S., 2017. A zinc chloride-doped adhesive facilitates sealing at the dentin interface: a confocal laser microscopy study. J. Mech. Behav. Biomed. Mater. 74, 35–42.
Wambier, D.S., dos Santos, F.A., Guedes-Pinto, A.C., Jaeger, R.G., Simionato, M.R., 2007. Ultrastructural and microbiological analysis of the dentin layers affected by caries lesions in primary molars treated by minimal intervention. Pediatr. Dent. 29, 228–234.
Wang, X., Liu, S., Li, M., Yu, P., Chu, X., Li, L., Tan, G., Wang, Y., Chen, X., Zhang, Y., Ning, C., 2016. The synergistic antibacterial activity and mechanism of multi-component metal ions-containing aqueous solutions against Staphylococcus aureus. J. Inorg. Biochem. 163, 214–220.